Available online at BCREC website: https://bcrec.id

Bulletin of Chemical Reaction Engineering & Catalysis, 16 (3) 2021, 517-524

Research Article

# In Search of Magnetic Properties of Samarium Cobalt ($Sm_2Co_{17}$) within a Low-Temperature Sintering Process

**P. Puspitasari[1,2,*], A. Muhammad[1], A.A. Permanasari[1,2], T. Pasang[3], S.M.S.N.S. Zahari[4], N.A. Ahmad[5]**

[1]*Department of Mechanical Engineering, Universitas Negeri Malang, Indonesia.*
[2]*Centre of Advanced Material and Renewable Energy, Universitas Negeri Malang, Indonesia.*
[3]*Department of Manufacturing and Mechanical Engineering and Technology, Oregon Institute of Technology, Klamath Falls, United States.*
[4]*Industrial Chemical Technology Programme, Universiti Sains Islam Malaysia, Bandar Baru Nilai, Negeri Sembilan, Malaysia.*
[5]*Department of Electrical and Electronics Engineering, Mahsa University, Selangor, Malaysia.*

*Received: 1st March 2021; Revised: 11th May 2021; Accepted: 11th May 2021*
*Available online: 28th May 2021; Published regularly: September 2021*

## Abstract

Samarium cobalt is known as super high density magnetic material with large magnetic anisotropy energy. Samarium–cobalt exhibits manipulative magnetic properties as a rare-earth material which has different properties in a low sintering temperature. It is therefore of paramount importance to investigate samarium cobalt ($Sm_2Co_{17}$) magnetic properties in the low temperature sintering condition. $Sm_2Co_{17}$, which is utilized in this research, is synthesized via the sol–gel process at sintering temperatures of 400, 500, and 600 °C. Subsequently, the crystallites indicate the formation of a single-phase $Sm_2Co_{17}$ on all the samples in all temperature variations. Moreover, the peaks in the X-ray diffraction analysis of crystallite sizes calculated using the Scherrer equation are 17.730, 15.197, and 13.296 nm at 400, 500, and 600 °C. Through scanning electron microscopy, the particles are found to be relatively large and agglomerated, with average sizes of 143.65, 168.78, and 237.26 nm. The functional groups are also analyzed via Fourier-transform infrared spectroscopy, which results in the appearance of several bonds in the samples, for example, alkyl halides, alkanes, and esters with aromatic functional groups on the fingerprint area and alkynes, alkyl halides, and alcohol functional groups at a wavelength of above 1500 cm. The test results of the magnetic properties using vibrating-sample magnetometer (VSM) revealed high coercivity and retentivity in the samples sintered at 400 °C. However, the highest saturation occurs in the samples sintered at 600 °C. At a low sintering temperature (below 1000 °C), samarium cobalt shows as the soft magnetic material.



***Keywords***: samarium-cobalt; sol-gel; sintering; magnetic properties; $Sm_2Co_{17}$

***How to Cite***: P. Puspitasari, A. Muhammad, A.A. Permanasari, T. Pasang, S.M.S.N.S. Zahari, N.A. Ahmad (2021). In Search of Magnetic Properties of Samarium Cobalt ($Sm_2Co_{17}$) within a Low-Temperature Sintering Process. *Bulletin of Chemical Reaction Engineering & Catalysis*, 16(3), 517-524 (doi:10.9767/bcrec.16.3.10482.517-524)

***Permalink/DOI***: https://doi.org/10.9767/bcrec.16.3.10482.517-524

## 1. Introduction

Generally, synthesis of rare-earth materials is carried out using complex methods and at extremely high sintering temperatures (over 1000 °C). Research on samarium cobalt as a rare earth metal has been a prevalent issue in the academia, particularly the investigations of the changes in its magnetic and physical properties at low sintering temperatures (below 1000 °C). Samarium-cobalt has very high magnetic properties, especially in terms of coercivity and magnetization saturation, and is greatly dependent

* Corresponding Author.
Email: poppy@um.ac.id (P. Puspitasari);
Telp: +6281231567675, Fax: +62-341-551312

on microscopic conditions, such as: the microstructure of the material, magnetic moments, and magnetic anisotropy. The magnetic properties can be controlled by adjusting the amount of cobalt in samarium. The development of nanotechnology has become prevalent and is one of the reasons for the increasing technological development. Researchers have attempted to determine and manipulate the nanomaterial properties according to their fields, one example being the magnetic nanoparticles. Magnetic materials have been widely used, *e.g.* for storage memory, sensor, and drug delivery [1–10]. Moreover, each material element can be developed and manipulated via nanotechnology.

Due to the limited number of rare-earth materials, they are difficult to find. However, they have high values as their properties are better compared with common material properties. Furthermore [11], these materials exhibit a manipulative property, which makes them easier to develop. In short, their properties are easier to change.

The magnetic properties of rare-earth materials largely influence the current technology and can be applied in mechanical, electrical, and medical fields. The examples of rare-earth materials exhibiting good magnetic properties are samarium and cobalt [12,13]. Theoretically speaking, Samarium-cobalt was developed as early as around 1960 based on the works carried out by Karl Strnat and Alden Ray at Wright-Patterson Air Force Base and University of Dayton. In particular, Strnat and Ray developed the first formulation of $SmCo_5$. They generally do not only have the same rating in strength of neodymium magnets, but also a higher temperature rating and a higher coercivity. However, it is brittle, easily cracked, and broken. Samarium-cobalt magnets have a maximum energy product (BHmax) that ranges from 16 Megagauss-Oersteds (MG.Oe) to 33 MG.Oe, which is approx. 128 kJ/m$^3$ to 264 kJ/m$^3$; and their theoretical limit is 34 MG.Oe, about 272 kJ/m$^3$. Sintered magnets on the Samarium-cobalt material exhibit magnetic anisotropy. Consequently, they can only be magnetized within their axis of magnetic orientation. This is done by aligning the crystal structure of the material during the manufacturing process. Samarium exhibits good sensitivity toward the magnetic field and is also temperature-resistant, whereas cobalt has a good magnetic energy storage.

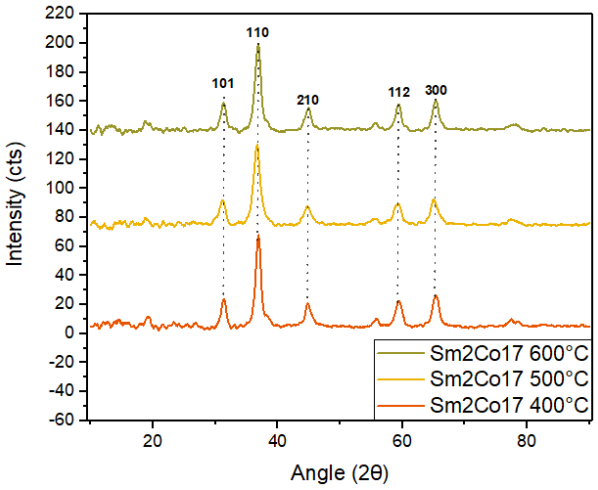


Figure 1. X-ray diffraction analysis result at various sintering temperatures.

Based on the above reasons, the researchers aimed to discover significant information to increase and manipulate samarium–cobalt via numerous processes. To obtain powdered samples with sintering temperatures of 400, 500, and 600 ℃, this research employed the sol–gel and sintering methods. The sol-gel method in the synthesis of samarium-cobalt has several advantages over other methods. In the sol-gel method, there is a phase change from the colloid suspension (sol) to form a continuous liquid phase (gel) in the vaporization process [14]. The two processes in the sol-gel method can increase the magnetic saturation value up to 80–120 emu/g [11,15,16]. Then, the sintering process is added at a certain temperature and in a certain holding time at the peak temperature it is able to produce a material with a large magnetic coercivity reaching 3.43 kOe [17,18].

## 2. Method and Materials

This research employed the sol–gel method to obtain results and factors influencing the physical and magnetic properties. This paper described how to manipulate and apply samarium–cobalt in numerous fields. In the sol–gel process, the materials were dissolved into molecules. Then, the compound was saturated to decompose the used solution and to form synthesized compounds from molecules to nanopowders [19,20].

After forming the nanopowders, sintering was conducted by heating the materials at 400, 500, and 600 ℃ under an open-air condition for sample atomization. The formation of crystallites indicated atomization. Then, posttreatment of powder underwent several material characterization tests.

Precursors in the form of cobalt(II) nitrate hexahydrate and samarium(III) nitrate hexahydrate powder were obtained from Sigma-

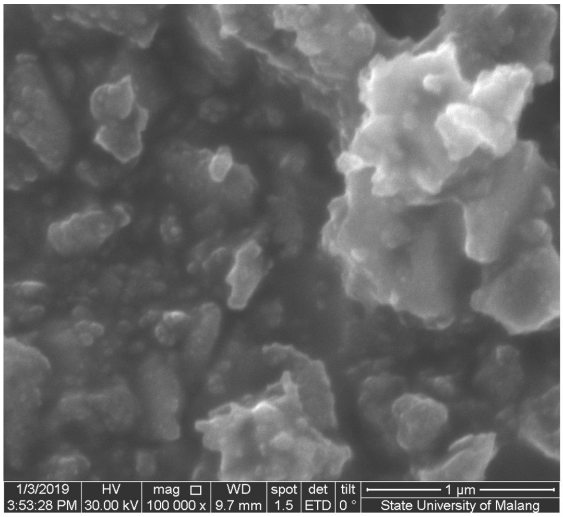


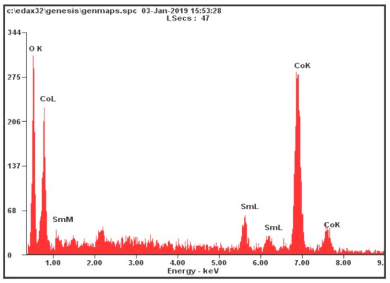


| Element | Wt% | At% |
|---|---|---|
| OK | 23.02 | 55.43 |
| SmL | 14.45 | 03.70 |
| CoK | 62.52 | 40.87 |
| Matrix | Correction | ZAF |

(a)

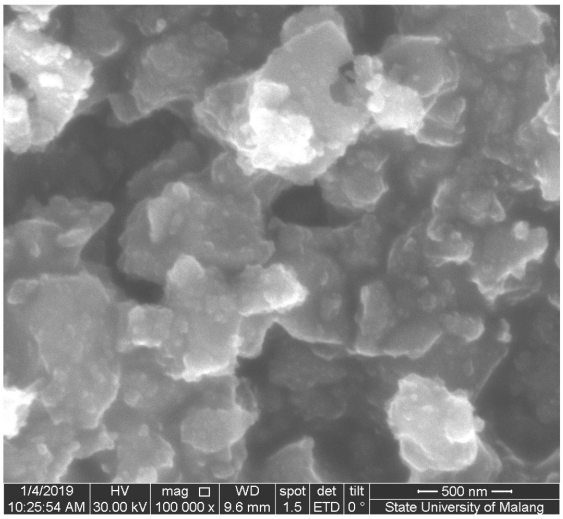


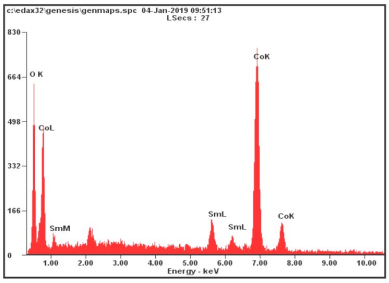


| Element | Wt% | At% |
|---|---|---|
| OK | 20.10 | 51.09 |
| SmL | 14.81 | 04.00 |
| CoK | 65.09 | 44.91 |
| Matrix | Correction | ZAF |

(b)

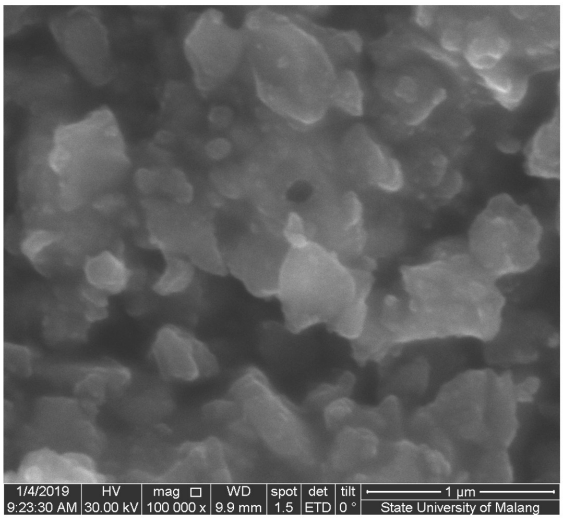


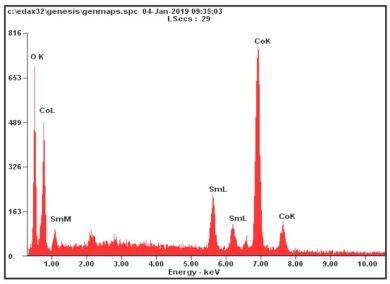


| Element | Wt% | At% |
|---|---|---|
| OK | 18.38 | 50.14 |
| SmL | 23.48 | 06.82 |
| CoK | 58.13 | 43.04 |
| Matrix | Correction | ZAF |

(c)

Figure 2 Morphological analysis of $Sm_2Co_{17}$ from the results of the SEM/EDX at various sintering temperature: (a) 400 °C, (b) 500 °C, and (c) 600 °C.

Aldrich (99% purity). To obtain $Sm_2Co_{17}$, the ratio of the samarium and cobalt precursors was set to 2:19. Ethylene glycol was added in the solution with a 1:3 ratio to the total amount of precursor. The samples were stirred using a magnetic stirrer for 2 h to dissolve the precursors. Subsequently, heat treatment was performed up to temperatures of 70–80 °C until the samples turned into gel. Then, the drying and crushing processes were initiated until the powder samples were obtained.

After the samples were synthesized via the sol–gel method, they were sintered at 400, 500, and 600 °C for 1 h to increase crystal formation. The samples were then tested via the following techniques: X-ray diffraction (XRD) microscopy (PanAnalytical Xpert Pro) with a long-range angle of 10°–90° 2θ to determine the crystallinity; scanning electron microscopy (SEM)/EDX (SEM with EDAX feature Model FEI, Inspect-S50) at a magnification of 100.000× to obtain the morphologies and nano-elements produced; Fourier-transform infrared spectroscopy (FTIR) (FTIR model, IRPrestige-21, Shimadzu) at a wavelength of 500–4000 cm to find the functional groups and bonds; and vibrating-sample magnetometry (VSM) (vibrating-sample magnetometer model, OXFORD, VSM 1.2H/CF/HT) up to 1 tesla of magnetic force to determine the magnetic coercivity, retentivity, or saturation in all the samples.

## 3. Results and Discussions

The XRD graphics presented below demonstrates that all the samples have five peaks: (101), (110), (210), (112), and (300). In other words, they formed a single-phase $Sm_2Co_{17}$ with crystallites. In summary, the temperature increases during heat treatment which is associated with the crystallite size of the nanoparticles is trivial. Heat treatment can improve crystallization, which, in turn, causes the grain size to increase [21]. The increment of grain size occurs as the influence of cobalt phase characteristics and the similar results also appeared in previous studies of cobalt crystallites [22,23]. Moreover, the lattice parameters of each sample have similar values and do not significantly change the temperature variations in the sintering process.

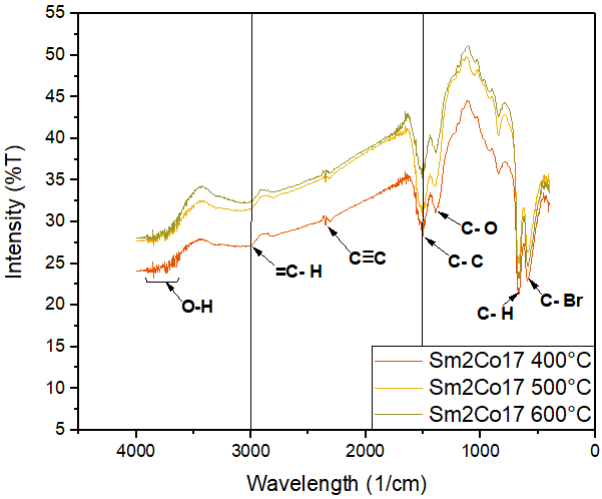


Figure 3. FTIR analysis of $Sm_2Co_{17}$ at various sintering temperatures.

Figure 1 shows that the cubical structure was observed at the highest peak (110). To measure the size of the crystallites, the Scherrer equation [24–26] was utilized as shown as Table 1. The samples heated at 400, 500, and 600 °C had crystallite sizes of 17.730, 15.197, and 13.296 nm, respectively. The decrease of crystallite size happened since there is a diminish grain in special condition, whereas the sintering of the powders with nanoparticles dimensions is performed. When sintering is performed with different stress, the inducement evokes different strain responding mechanism.

From the results of the SEM/EDX, Figure 2(a) presents the samples sintered at 400 °C; Figure 2(b), the samples sintered at 500 °C; and Figure 2(c), the samples sintered at 600 °C. Generally, all the samples had similar morphologies. The nanopowders were found to be agglomerate and forming clusters that contain nanobulks. Such occurrence indicated that the internal magnetic force of $Sm_2Co_{17}$ is sufficient to enable bonding among the particles. Moreover, the emergence of some large-sized particles was due to particle unification during sintering [21]. The average sizes of the particles were 143.65, 168.78, and 237.26 nm at 400, 500, and 600°C, respectively, which were calculated using the ASTM standard method.

The results of the FTIR presented in Figure 3 reveal several bonds in the samples. The discovery of alkyl halides, alkanes, esters, and aromatic (C−Br), (C−H), (C−O), and (C−C) functional groups in the fingerprint area found at a wavelength of 0–1500 cm. Moreover, (C=C), (=C−H), and (O−H) bonds, which are alkynes, alkyl halides, and alcohol functional groups, were observed above the wavelength of 1500 cm. The appearance of these bonds was due to the reduction process from the imperfect synthesis during the sol–gel process, thus leaving several impurities from the used solution [27]. No varieties in the peaks of the samples were observed, only declining intensity and increasing temperatures.

The VSM test was conducted to obtain three magnetic properties: magnetic saturation, the ability to generate magnetic force as long as the material obtains the external magnetic field; magnetic retentivity, the ability to store magnetic energy that is converted to internal magnetic force after obtaining the external magnetic field; and coercivity, the value that determines the amount of magnetic field required to diminish the internal magnetic force from a material.

Figure 4 demonstrates the highest saturation value from the samples sintered at 600 ℃, namely, 0.457 emu/g, and classified as superparamagnetic. However, retentivity and coercivity only appeared in the samples sintered at 600 ℃, with 0.003 emu/g and 0.015 T, as presented in Table 2. This occurrence was induced by the imperfect formation of crystallites at 500 ℃ and 400 ℃. The results also called by non-hysteresis condition with zero coercivity and retentivity, which indicated that the sample exhibits an isotropic characteristic without a preferential axis [27]. Moreover, it indicates that under a normal sintering temperature, the material temperatures of 500 °C and 400 ℃ exhibit ferromagnetic properties with a magnetic saturation of 0.219 and 0.239 emu/g [27–29]. In the magnetic nanoparticles, the particle size significantly influences the magnetic strength [18]. The particle size also greatly influences the magnetic force in the magnetic nanoparticles [18]. Even though the sintering process causes crystallization, the size of the particles will increase [21] and cause lower magnetic properties compared with bulk alloy materials.

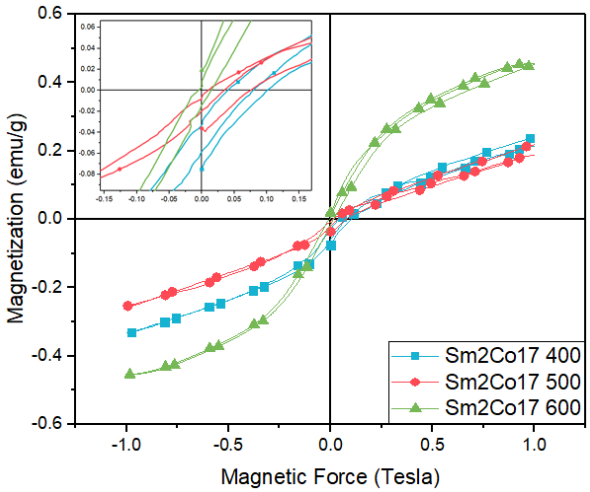


Figure 4. Hysteresis curve comparison of $Sm_2Co_{17}$ at different sintering temperatures.

There are 3 theories about the phenomena of changing magnetic behavior that take place. First, there is super-exchange interaction which is a change in the magnetic moment caused by a change in the direction of the electron spin because it is affected by atomic elements which have a more dominant spin moment when the formulas of the two elements are combined with the composition different. This causes the material to be ferromagnetic and paramagnetic when it is not energized by an external magnetic field. The mechanism is shown in Figure 5.

Second, there is hyperfine coupling [30,31] which occurs because during the heating process the atoms are reactive with random movements causing some of the electron spins of the outer shell of the atom to have their own magnetic moment direction and affect the magnetic moment of the atomic nucleus. This causes the material to be able to turn superparamagnetic and antiferromagnetic when it is not energized by an external magnetic field.

The third is the Zeeman Effect [32,33] which has 2 types, the first is the effect of an external magnetic moment which only affects the atomic nucleus, causing the magnetic mo-

Table 1. Crystallinity analysis of $Sm_2Co_{17}$ from the XRD result in (110).

| Temperature (°C) | Pos. [°2θ] | Height (cts) | FWHM [°2θ] | *d*-spacing (Å) | Crystallite Size (nm) |
|---|---|---|---|---|---|
| 400 | 36.86 | 49.38 | 0.5510 | 2.4381 | 17.730 |
| 500 | 36.88 | 68.01 | 0.4723 | 2.4371 | 15.197 |
| 600 | 36.88 | 55.46 | 0.6298 | 2.4370 | 13.296 |

Table 2. Analysis of the magnetic properties of $Sm_2Co_{17}$ based on the VSM graphics.

| Temperature (°C) | *Hc* (T) | *Mr* (emu/g) | *M*s (emu/g) |
|---|---|---|---|
| 400 | 0 | 0 | 0.239 |
| 500 | 0 | 0 | 0.219 |
| 600 | 0.015 | 0.003 | 0.457 |

ment to be zero. The second type is when an external magnetic moment is applied which causes a change in the spectral line/electron trajectory caused by an external magnetic field so that it can change the direction of the electron spin rotation so that the magnetic moment changes to follow or reject the direction of the external magnetic field.

## 4. Conclusions

The XRD analysis revealed the formation of a single-phase $Sm_2Co_{17}$ indicated by the crystallite peaks. The analysis also concluded that the increase in temperatures led to the formation of smaller-sized crystallites. Furthermore, the SEM analysis portrayed the particle morphologies of uniting and agglomerate particles that form clusters in all the samples with average sizes of 143.65, 168.78, and 237.26 at 400, 500, and 600 ℃, respectively. In addition to the XRD and SEM results, the FTIR analysis discovered several bonds in the samples, for example, alkyl halides, alkanes, esters, and an aromatic functional group at the fingerprint and then alkynes, alkyl halides, and alcohol functional groups above the wavelength of 1500 cm. Lastly, the VSM analysis exhibited the highest saturation was observed in the samples sintered at 600 ℃. Through the low-temperature sintering process, samarium–cobalt was found to exhibit the properties of a soft magnetic material.

## Acknowledgement

Authors would like to thank Ministry of Education, Culture, Research and Technology Republic of Indonesia (Kemendikbud-Ristek) and BRIN for PDUPT grant with contract number 10.3.90/UN32.14.1/LT/2020.

## References

[1] Zhuang, M., Wang, L., Wu, G., Wang, K., Jiang, X. (2017). Health risk assessment of rare earth elements in cereals from mining area in Shandong, China. *Scientific Reports*, 7, 9772. DOI: 10.1038/s41598-017-10256-7

[2] Yang, C., Jia, L., Wang, S., Gao, C., Shi, D., Hou, Y., Gao, S. (2013). Single Domain SmCo5@Co Exchange-coupled Magnets Prepared from Core/shell $Sm[Co(CN)_6].4H_2O$@GO Particles: A Novel Chemical Approach. 1–7. DOI: 10.1038/srep03542

[3] Wu, L., Mendoza-garcia, A., Li, Q., Sun, S. (2016). Organic Phase Syntheses of Magnetic Nanoparticles and Their Applications. *Chemical Reviews*, 116(18), 10473–10512. DOI: 10.1021/acs.chemrev.5b00687

[4] Yue, M., Zhang, X., Liu, J.P. (2017). Fabrication of bulk nanostructured permanent magnets with high energy density: Challenges and approaches. *Nanoscale*, 9, 3674-3697. DOI: 10.1039/C6NR09464C

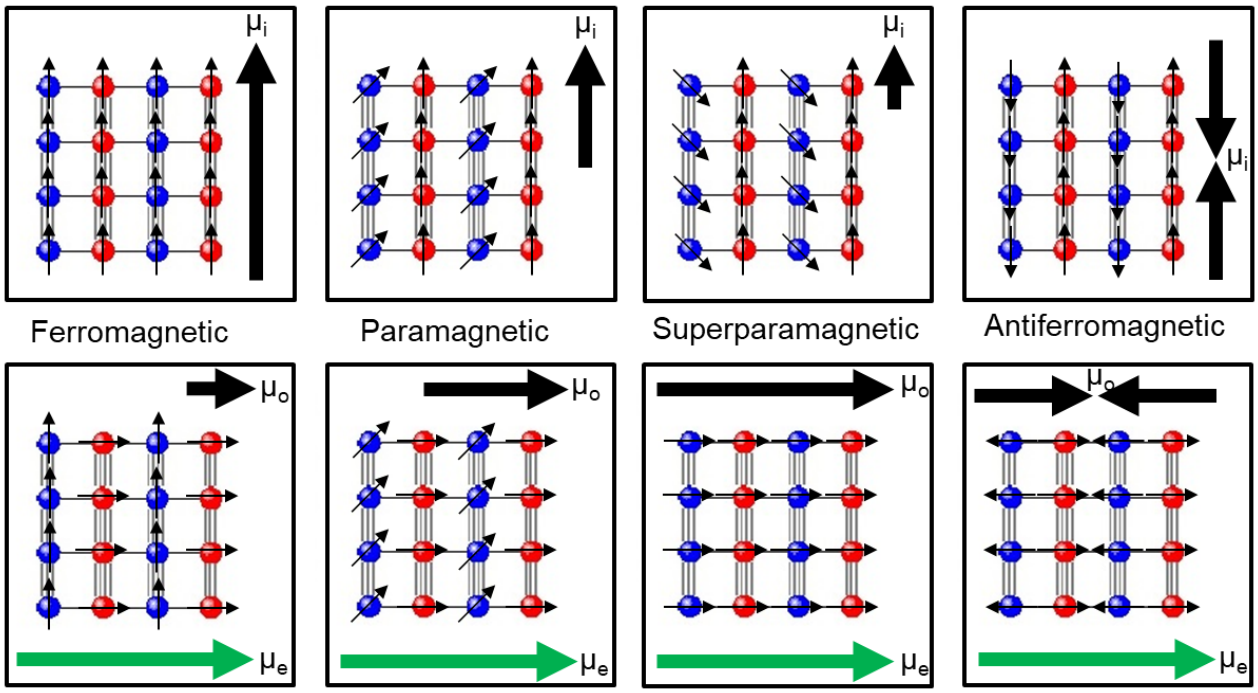


Figure 5. The mechanism of superexchange interaction

[5] Xiong, Y., Xianmao, L. (2015). *Metallic Nanostructures*. Springer International Publishing. DOI: 10.1007/978-3-319-11304-3

[6] Ai, Y., Liu, Y., Lan, W., Jin, J., Xing, J., Zou, Y., Zhao, C., Wang, X. (2018). The effect of pH on the U(VI) sorption on graphene oxide (GO): A theoretical study. *Chemical Engineering Journal*, 343, 460–466. DOI: 10.1016/j.cej.2018.03.027

[7] López-Ortega, A., Estrader, M., Salazar-Alvarez, G., Roca, A.G., Nogués, J. (2015). Applications of exchange coupled bi-magnetic hard/soft and soft/hard magnetic core/shell nanoparticles. *Phys. Rep*. 553, 1-32. DOI: 10.1016/j.physrep.2014.09.007

[8] Liu, F., Hou, Y., Gao, S. (2014). Exchange-coupled nanocomposites: Chemical synthesis, characterization and applications. *Chemical Society Reviews*, 43, 8098–8113. DOI: 10.1039/C4CS00162A

[9] Ma, Z., Zhang, T., Jiang, C. (2015). Exchange-coupled $SmCo_5$/Co nanocomposites synthesized by a novel strategy. *RSC Advances*, 5(c), 89128–89132. DOI: 10.1039/C5RA15079E

[10] Ma, Z., Yang, S., Zhang, T., Jiang, C. (2016). The chemical synthesis of $SmCo_5$ single-crystal particles with small size and high performance. *Chemical Engineering Journal*, 304, 993–999. DOI: 10.1016/j.cej.2016.07.024

[11] Suresh, G., Saravanan, P., Babu, D.R. (2012). Effect of annealing on phase composition, structural and magnetic properties of Sm-Co based nanomagnetic material synthesized by sol-gel process. *Journal of Magnetism and Magnetic Materials*, 324(13), 2158–2162. DOI: 10.1016/j.jmmm.2012.02.038

[12] Khan, Y. (1972). A Contribution to the Sm-Co Phase Diagram. *Acta Crystallographica, Section B, Structural Science*, 290–292. DOI: 10.1107/S0567740874003943

[13] Ray, A.E. (1972). *Research and Development of Rare Earth Transition Metal Alloys as Permanent Magnet Materials*. AD0774471

[14] Bu, S., Duan, X., Han, X., Sun, J., Chi, X., Cui, C. (2016). Preparation , microstructure and magnetic properties of Sm(Co,Hf)7/Co nanocomposite particles by polyol method ( f ) (g). *Physica B: Physics of Condensed Matter*, 506, 138–144. DOI: 10.1016/j.physb.2016.11.010

[15] Chem, J.M., Zhang, H., Peng, S., Rong, C., Liu, J.P., Zhang, Y., Kramer, M.J. (2011). Chemical synthesis of hard magnetic SmCo nanoparticles. *Journal of Materials Chemistry*, 21, 16873–16876. DOI: 10.1039/c1jm11753j

[16] Lee, J., Hwang, T.-Y., Kang, M.K., Cho, H.-B., Kim, J., Myung, N.V., Choa, Y.-H. (2018). Synthesis of Samarium-Cobalt Sub-micron Fibers and Their Excellent Hard Magnetic Properties. *Frontiers in Chemistry*, 6, 1–7. DOI: g/10.3389/fchem.2018.00018

[17] Saravanan, P., Premkumar, M., Singh, A.K., Gopalan, R., Chandrasekaran, V. (2009). Study on morphology and magnetic behavior of $SmCo_5$ and $SmCo_5$/Fe nanoparticles synthesized by surfactant-assisted ball milling. *Journal of Alloys and Compounds*, 480, 645–649. 10.1016/j.jallcom.2009.01.129

[18] Wu, W., Zhang, J., Cao, P., Dong, J., Ding, H. (2018). Synthesis of Sm–Co nanoparticles by sol–gel method. *Modern Physics Letters B*, 32, 1840069. DOI: 10.1142/S0217984918400699

[19] Dehghanghadikolaei, A., Ansary, J., Ghoreishi, R. (2018). Sol-gel process applications: A mini-review. *Proceedings of the Nature Research Society*, 2, 02008. DOI: 10.11605/j.pnrs.201802008

[20] Xavier, S., Thankachan, S., Jacob, B.P., Mohammed, E.M. (2013). Effect of Samarium Substitution on the Structural and Magnetic Properties of Nanocrystalline Cobalt Ferrite. *Journal of Nanoscience*, 2013, 524380. DOI: 10.1155/2013/524380

[21] Tian, J., Zhang, S., Qu, X., Pan, D., Zhang, M. (2012). Co-reduction synthesis of uniform ferromagnetic SmCo nanoparticles. *Materials Letters*, 68, 212–214. DOI: 10.1016/j.matlet.2011.10.076

[22] Acosta-Humánez F., Almanza O., Vargas-Hernández, C. (2014). Effect of sintering temperature on the structure and mean crystallite size of Zn1-xCoxO (x = 0.01 - 0.05) samples. *Superficies y Vacio* 27(2), 43–48. http://www.scielo.org.mx/pdf/sv/v27n2/v27n2a2.pdf

[23] Saravanan, P., Gopalan, R., Sivaprahasam, D., Chandrasekaran, V. (2009). Intermetallics Effect of sintering temperature on the structure and magnetic properties of $SmCo_5$/Fe nanocomposite magnets prepared by spark plasma sintering. *Intermetallics*, 17(7), 517–522. DOI: 10.1016/j.intermet.2009.01.005

[24] Razak, J.A., Sufian, S., Ku Shaari, K.Z., Puspitasari, P., Hoe, T.K., Yahya, N. (2012). Synthesis, characterization and application of $Y_3Fe_5O_{12}$ nanocatalyst for green production of $NH_3$ using magnetic induction method (MIM). *AIP Conference Proceedings*, 1482, 633–638. DOI: 10.1063/1.4757548

[25] Yahya, N., Puspitasari, P. (2012). $Y_3Fe_5O_{12}$ Nanocatalyst for Green ammonia Production by Using Magnetic Induction Method. Journal *of Nano Research*, 21, 131–137. DOI: 10.4028/www.scientific.net/JNanoR.21.131

[26] Puspitasari, P. (2016). Green Ammonia Synthesis using Nanocatalysts in a Novel Magnetic Induction Method (MIM). *Doctoral Thesis*. Electrical and Electronic Engineering Department, University Technology PETRONAS, Malaysia.

[27] Bastl, Z., Subrt, J., Bakardjieva, S., Bezdiˇ, P. (2011). Chemistry IR laser deposition: $Co_2Sm_5$ nanocrystals in amorphous Sm – Co phase and amorphous Sm – Co nanobodies in carbonaceous phase. *Journal of Photochemistry and Photobiology A: Chemistry*, 223, 132–139. DOI: 10.1016/j.jphotochem.2011.08.010

[28] Panzeri, G., Tresoldi, M., Rinaldi, C., Magagnin, L. (2017). Electrodeposition of Magnetic SmCo Films from Deep Eutectic Solvents and Choline Chloride-Ethylene Glycol Mixtures. *Journal of The Electrochemical Society*, 164(13), 2017–2020. DOI: 10.1149/2.0111714jes

[29] Iván, C., Rodríguez, R., Rurik, J., Mancilla, F., Edith, K., Chavez, V., Magaña, F.E., Federico, S., Méndez, O., Trinidad, J., Galindo, E. (2015). Effect of Thickness on Magnetic Dipolar and Exchange Interactions in SmCo/FeCo/SmCo Thin Films. *Advances in Materials Physics and Chemistry*, 5(9), 368–373. DOI: 10.4236/ampc.2015.59037

[30] Onodera, H., Yamaguchi, Y., Yamamoto, H., Sagawa, M., Matsuura, Y., Yamamoto, H. (1984). Magnetic properties of a new permanent magnet based on a Nd-Fe-B compound (neomax). I. Mössbauer study. *Journal of Magnetism and Magnetic Materials,* 46(1–2), 151–156. DOI: 10.1016/0304-8853(84)90352-4

[31] Medina M., Cammack, R. (2007). Endor and Related EMR Methods Applied to Flavoprotein Radicals. *Applied Magnetic Resonance*, 31, 457-470. DOI: 10.1007/BF03166596

[32] Ozerov, R.P., Vorobyev, A.A. (2007). Elements of Quantum Mechanics. In *Physics for Chemists*, Elsevier B.V., 423–496. DOI: 10.1016/b978-044452830-8/50009-x

[33] Puspitasari, P., Andoko, A., Suryanto, H., Risdanareni, P., Ekaputri, J.J. (2017). Properties of $Mn_{0.4}Zn_{0.6}Fe_2O_4$ and $Mn_{0.6}Zn_{0.4}Fe_2O_4$ as Nanocatalyst for Ammonia Production. *MATEC Web of Conferences*, 97, 01029. DOI: 10.1051/matecconf/20179701029

*Selected and Revised Papers from International Conference on Sustainable Energy and Catalysis 2021 (ICSEC 2021) (https://engineering.utm.my/chemicalenergy/icsec2021/) (School of Chemical and Energy Engineering, Faculty of Engineering, Universiti Teknologi Malaysia, 16-17th February 2021) after Peer-reviewed by Scientific Committee of ICSEC 2021 and Peer-Reviewers of Bulletin of Chemical Reaction Engineering & Catalysis.*
*Editors (Guest) in this ICSEC 2021 section are Nor Aishah Saidina Amin, Mohd Asmadi Mohammed Yussuf, Salman Raza Naqvi, while Editor in Chief is I. Istadi.*